Science Advances
AAAS

advances.sciencemag.org/cgi/content/full/5/6/eaav3809/DC1

Supplementary Materials for

Central Europe temperature constrained by speleothem fluid inclusion water isotopes over the past 14,000 years

Stéphane Affolter*, Anamaria Häuselmann, Dominik Fleitmann, R. Lawrence Edwards, Hai Cheng, Markus Leuenberger

*Corresponding author. Email: affolter@climate.unibe.ch

Published 5 June 2019, *Sci. Adv.* **5**, eaav3809 (2019)
DOI: 10.1126/sciadv.aav3809

This PDF file includes:

Supplementary Text

Extended temperature discussion

For fluid inclusion samples, ages given in the following text correspond to the mean age of the sample interval. After the Allerød (mean MC-FIT of 4.9 ± 0.3 °C), the beginning of the YD is marked by a mean MC-FIT drop of 4.3 ± 0.8 °C, it is 2.9 °C for Mediterranean Sea surface temperature (SST) *(23)* and 7.5 °C for GISP2 *(10)*. YD exhibits a mean MC-FIT of 0.6 ± 0.5 °C with one interval close to zero degree (centered on 11976 BP). The transition to the Holocene is marked with a mean MC-FIT warming of 5.4 ± 0.7 °C to reach ~6.0 °C (11650-11366 BP) whereas mean SST and Greenland increases are 4.2 ° C and 12.5 °C respectively. In addition, summer temperatures based on European chironomids *(22)* show a similar shift to MC-FIT at the YD-Holocene onset. Early Holocene temperature rise is simultaneous and similar between MC-FIT (11650-9587 BP) and SST (11622-9589 BP) with rates of 1.34 ± 0.16 °C/1000 years and 1.32 ± 0.17 °C/1000 years respectively whereas it is 3.73 ± 0.01°C/1000 years for Greenland (11620-9550 BP). This warming is on average 2.8 °C for MC-FIT, 2.7 °C for SST and 7.7 °C for GISP2 and ends with the warmest Holocene multi-decades (9.6 ± 0.3 °C, 9588 BP) that is 1.3 °C warmer than recent times (RT = 1930-2011; 8.3 °C at Fahy station, 596 m a.s.l.). After the initial Holocene warming, the minimal MC-FIT Holocene value occurring at 11366 ± 149 BP (5.4 ± 0.4 °C) is synchronized within age uncertainty with Greenland (11271 ± 30 BP). The Holocene Thermal Maximum (HTM, ~9836 BP – 6417 BP in our record) was the only period with temperatures equal or warmer than the 21th century and more generally values are higher than for the last 4 ka BP. HTM shows a stable mean MC-FIT of 8.6 ± 0.1 °C for intervals 9836-8792 BP and 7787-6468 BP that coincides with warmest SST and Greenland periods interrupted by a cooler interval - the 8.2 ka event - that is well imprinted in the speleothem record with a sudden 1.2 ± 0.5 °C drop in temperature. It is in excellent agreement with regional temperature estimates of 1.2 °C in Bunker Cave, Germany *(27)*. Temperature reconstruction from lake Ammersee shows a drop of 1.7°C *(18)*. Pollen-based temperature reconstructions document a decrease of 1.5-2.0 °C in Europe *(52)*. The coldest part of 8.2 ka event in MC-FIT is followed by a rapid recovery and after a short stabilisation by an additional abrupt ~0.8 °C increase (in total 2.1 ± 0.5 °C) that leads to a stable warm state between 7787 and 6468 BP. Cold events that interrupt the early Holocene are synchronized with Greenland temperature minima at 11.5, 11.0, 9.3 and 8.2 ka BP, whereas the comparison for the mid-Holocene cold events is less significant, even if MC-FIT minima are also seen at 6.4, 5.9, 5.3 and 4.2 ka BP, but not at 7.2 ka BP. After the 8.2 ka event, there is a long-term gradual cooling between 7787 and 1906 years BP (ΔT of ~0.70 °C) at a mean rate of -0.12 ± 0.01 °C/1000 years with internal centennial to millennial scale variations in the order of 0.7 °C. The cooling trend for SST is similar (-0.13 ± 0.03 °C/1000 years, ΔT of ~0.77 °C, 7821-1898 BP) whereas it is -0.18 ± 0.01 °C/1000 years in Greenland (ΔT of ~1.06 °C, 7800-1900 BP). The last 3 ka BP are particularly well documented in our record with alternating cold and warm phases (fig. S8). Compared to RT, the Iron Age cold epoch (mean MC-FIT of 7.8 ± 0.1 °C) was ~0.5 °C colder. The beginning of the following Roman Warm Period (RWP) shows fairly constant mean MC-FIT of 8.1 ± 0.1 °C (2309-2077 BP) and 8.2 ± 0.1 °C (1773-1535 BP) interrupted by a 240 years colder phase (mean MC-FIT of 7.7 ± 0.1 °C). This cold phase is not seen in Greenland but coincides with a summer temperature trend of Lake Gemini, northern Italy *(9)*, which indicates a regional signature. After the RWP, a ~0.4 °C (from 8.2 to 7.8 °C) long-term trend "Dark ages" cooling is observed between 1472 and 1091 BP also coinciding with glacier advance in Europa *(53)*. The succeeding medieval climate anomaly (MCA) exhibits a ~0.4 °C warming to reach a mean MC-FIT of 8.2 ± 0.1 °C. The little ice age (LIA) interrupts the ongoing warm period with a ~40 years abrupt 1.5 ± 0.5 °C cooling starting at 694 BP to reach a MC-FIT minimum

of 7.2 ± 0.3 °C at 651 BP (1.1 °C cooler than RT). A mean 0.4 ± 0.2 °C MC-FIT cooling occurred between the MCA and the coldest part of the LIA (651-347 BP, 7.8 ± 0.1 °C). MC-FIT timing and amplitude of the LIA cooling is similar to the cooling of 0.5 °C in mean summer temperature (675-700 BP) based on the ice-cap growth from Canada-Arctic and Iceland *(28)*. Furthermore, a comparison with instrumental and reconstructed temperatures going back to 1500 CE (450 BP) *(29)* retrieved for the Milandre Cave grid cell (47-48° N / 6.5-7.5° E) is in very good agreement with our independent MC-FIT record (Fig. R1B). Finally, a comparison with instrumental temperatures from Switzerland (Basel) going back to 1755 CE (195 BP) (available on http://www.euroclimhist.unibe.ch/) shows a high degree of similarity with our MC-FIT reconstruction (fig. S9). During the current warming period, the interval 1990-2010 CE (-40 to -60 BP) exhibits a 1.2 °C increase compared to the mean of 1960-1990 CE (-10 to -40 BP) based on the MeteoSwiss instrumental temperatures record from the nearby Basel station. It is noteworthy that when looking at the trend between 10.5 to 0.5 ka as done by Ref. *(4)* for the pollen data set, the MC-FIT and NGRIP ice core show also a warming of ~0.7 °C and ~2 °C, respectively but these are in disagreement to regional pollen records close to Switzerland (fig. S7).

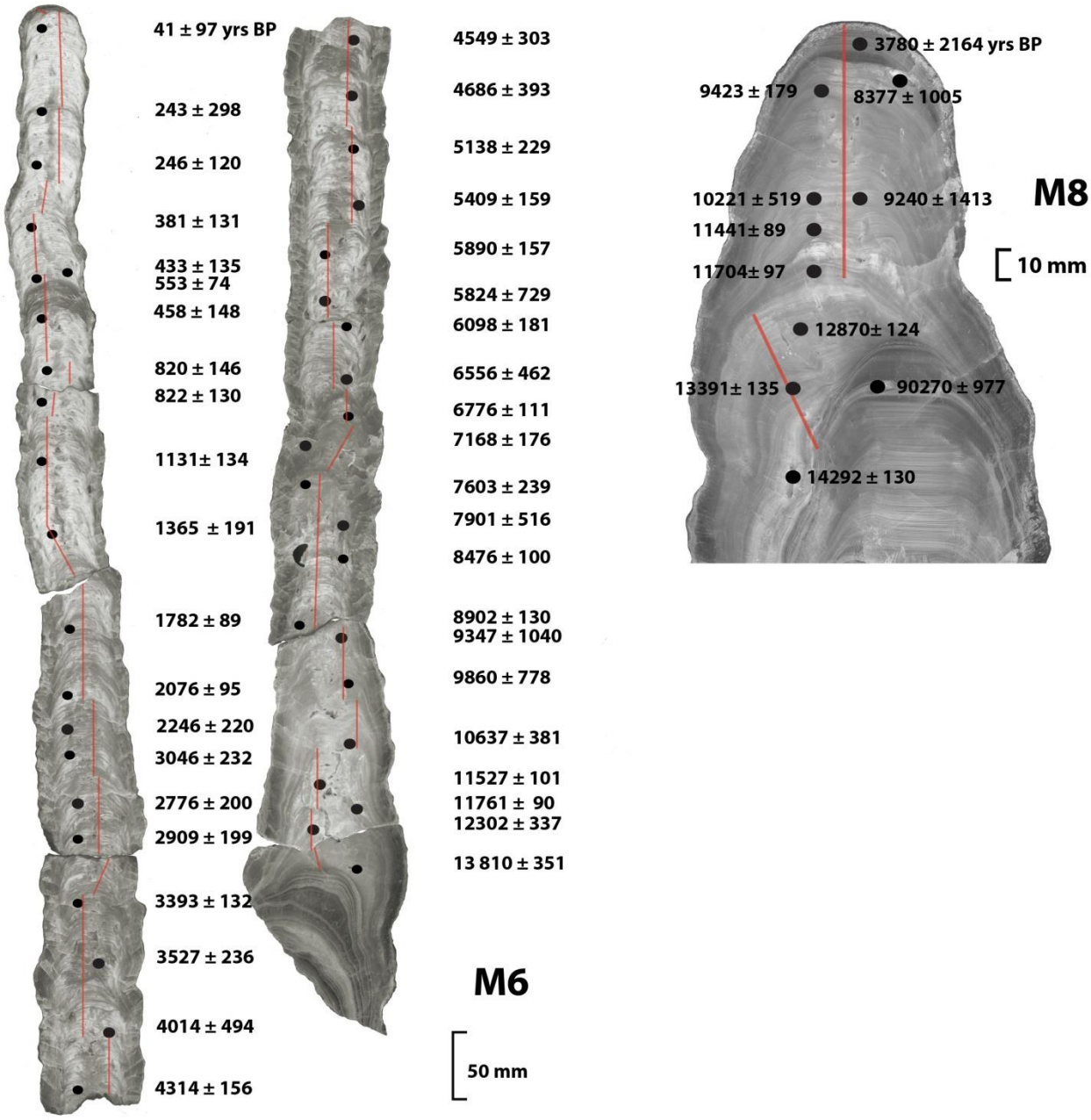

Fig. S1. Stalagmites M6 and M8 with U-Th age locations. Polished sections of M6 (length of 145.20 cm, left panel) and M8 (length of 13.25 cm, right panel) stalagmites made of compact columnar calcite. Both stalagmites grew several centimetres apart on the same calcite base (dated as Marine Isotope Stage 5 calcite). For M8, well-defined corrosion laminae mark the hiatus between the two calcite generations (between ages 90270 and 14292 years BP). A second major hiatus is visible above the studied section (between ages 3780 and 8377 years BP). Annual laminations are visible macroscopically and/or microscopically on M6 entire length, whereas for M8 laminations are visible only microscopically. Micromilling path for δ^{18}Oc isotopic analysis (red lines) shows several shifts in the growth axis position.

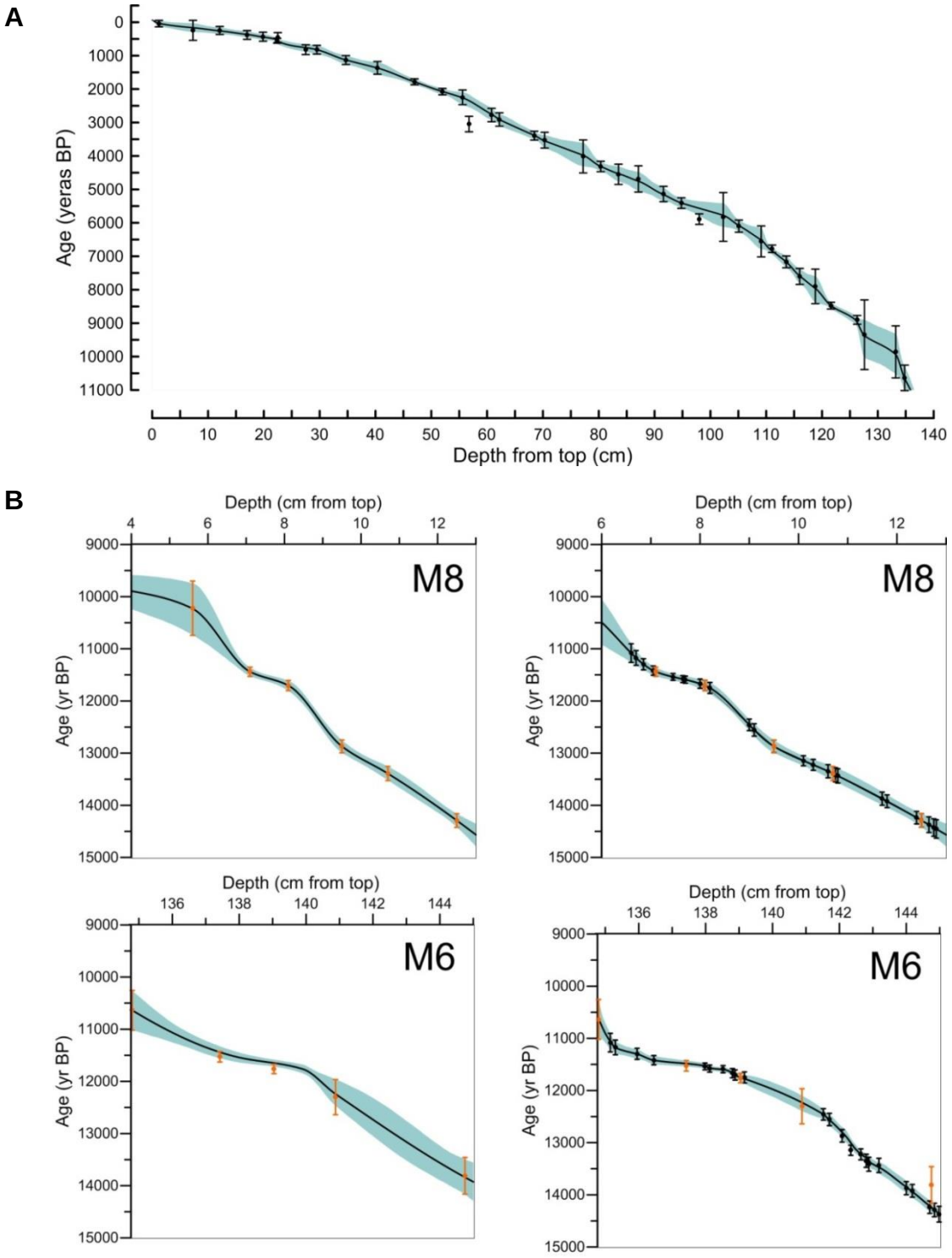

Fig. S2. Depth-age models for M6 and M8 stalagmites. (**A**) Depth-age model for M6. (**B**) Left side: individual depth-age models. Right side: depth-age models after the tuning. The outer shaded zones define the 95% uncertainties (2 sigmas). Measured (orange) and tuned (black) ages are represented. Note the different depth scale for sample M8.

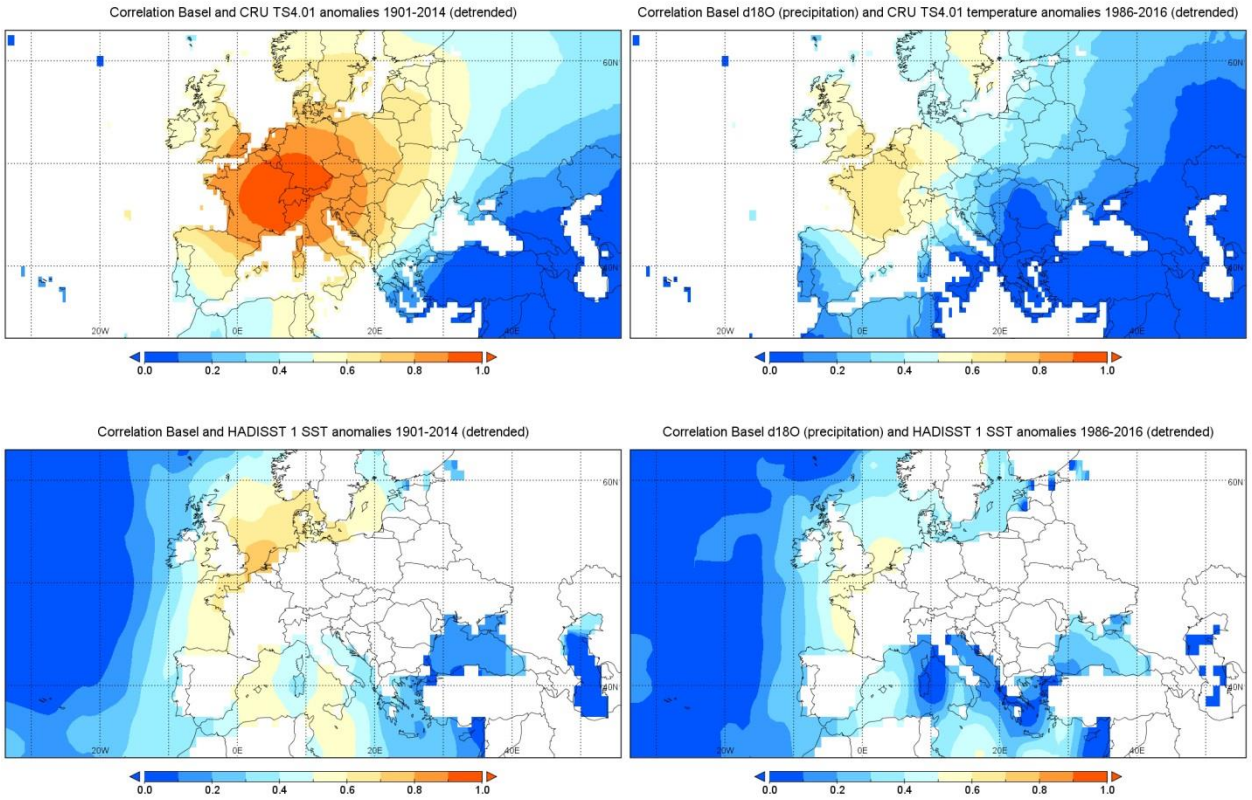

Fig. S3. Spatial correlation maps for temperatures and isotopes. Basel MeteoSwiss station temperature versus (**A**), European temperature and (**B**) SST for the period 1901-2014. Precipitation $\delta^{18}O_p$ at Basel station versus (**C**) European temperatures and (**D**) SST for the period 1986-2016. Maps were drawn using the KNMI climate explorer (http://climexp.knmi.nl). The seasonal cycle was removed and the records detrended prior to correlations with the CRU TS 4.01 dataset for atmospheric temperature *(54)* and HadISST1 dataset for SST *(55)*.

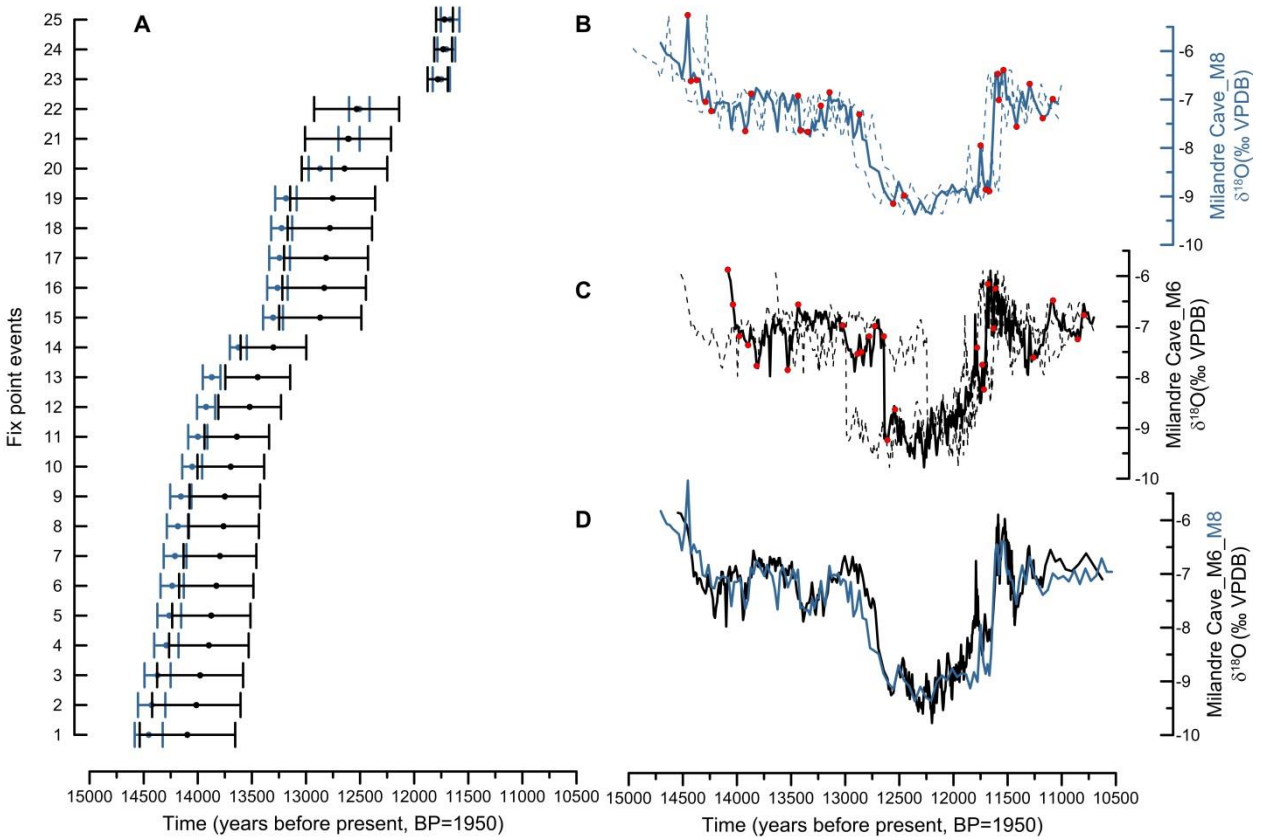

Fig. S4. Original $\delta^{18}O$ time series for M6 and M8 stalagmites. (**A**) Individual ages and errors of each fix points (red dots on the isotopic plots) chosen for final age model – tuning. (**B, C**) Original $\delta^{18}O$ time series for M6 (black) and M8 (blue) and location of "tuned points" (red dots). The outer dashed lines define the 95% uncertainties with individual dating results and errors. (**D**) Tuned stable isotopic time series of M6 (black) plotted together with the original isotopic time series of M8 (blue).

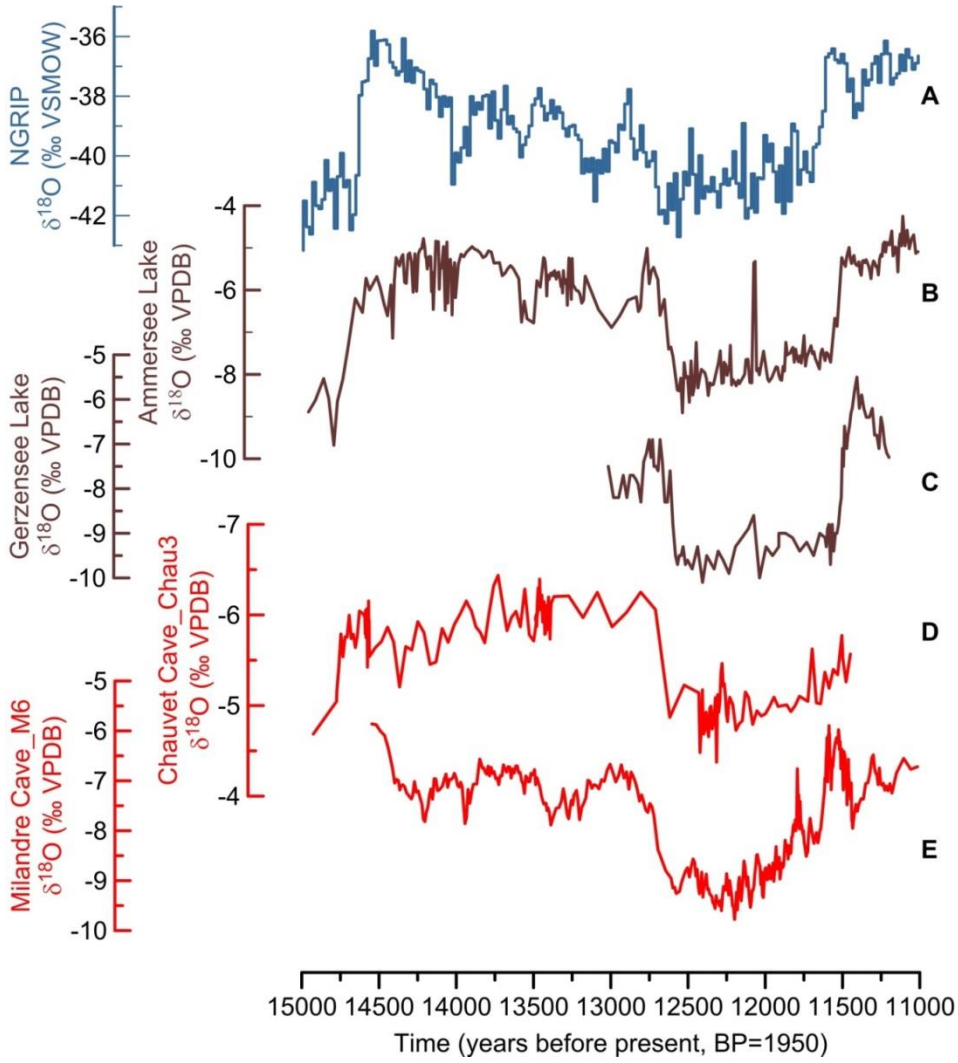

Fig. S5. Timing of Milandre Cave calcite $\delta^{18}O_c$ shifts (E) compared with other oxygen records. (**A**) NGRIP Greenland ice core *(21)*. (**B**) Lake Ammersee *(18)*. (**C**) Lake Gerzensee *(19)*. (**D**) Chauvet Cave *(56)*.

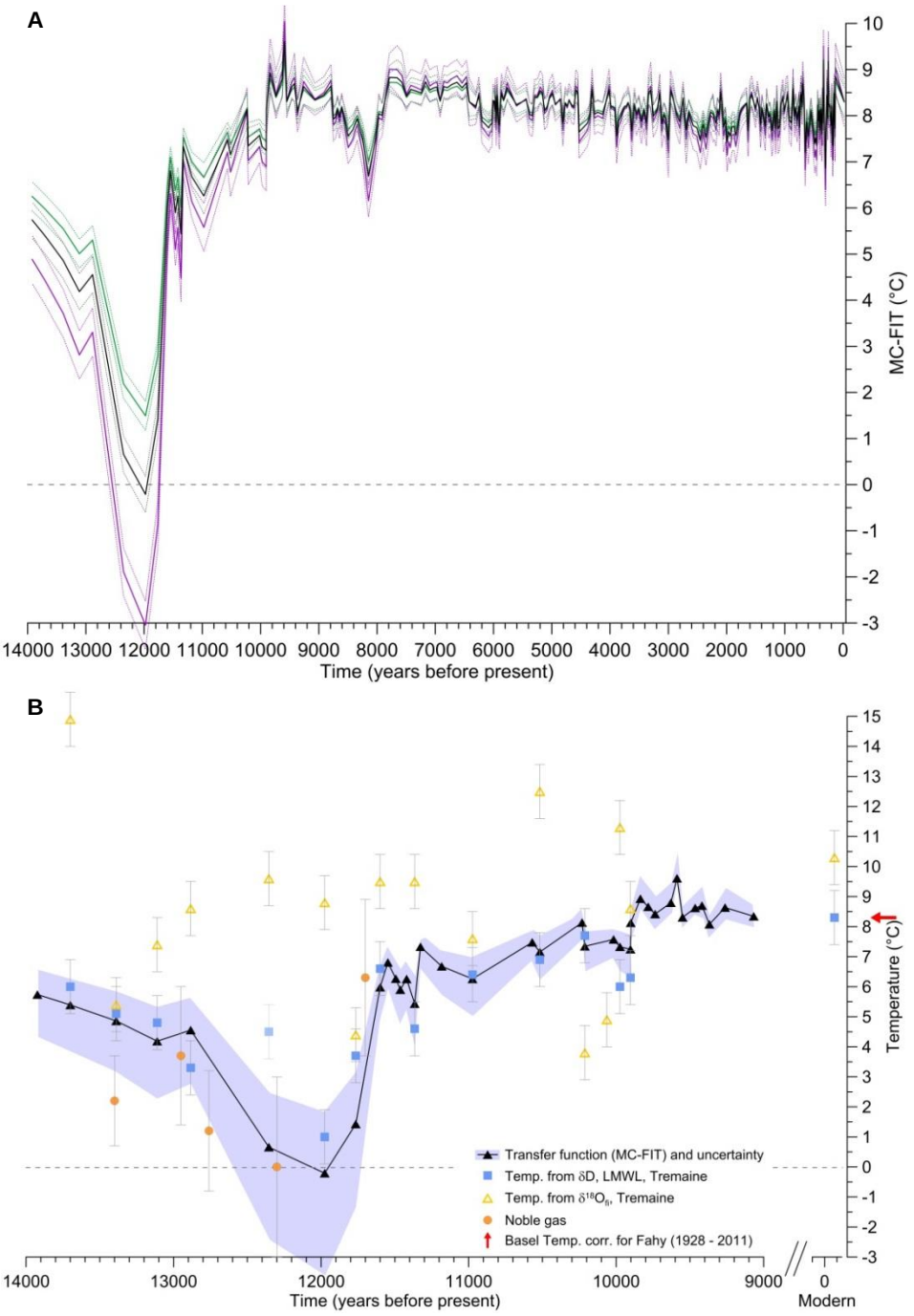

Fig. S6. Temperature reconstruction (MC-FIT) and uncertainties from speleothem fluid inclusions. (**A**) Transfer function of 0.48 ‰/ 1 °C (black), 0.36 ‰/ 1 °C (violet) and 0.60 ‰/ 1 °C (green) using δD_{fi} and corresponding measurement uncertainties (dotted lines). Shaded area given in Figs. 2 and 3 and figs. S6, S7 and S8 correspond to the maximal extent of conservative uncertainties. (**B**) Zoom on the Younger Dryas and modern interval using different temperature reconstructions that are (i) the MC-FIT (black triangle), the oxygen calcite-water thermometry using the measured δD_{fi} and LMWL *(25, 15)* to estimate the $\delta^{18}O_{fi,cal}$ (blue squares) or $\delta^{18}O_{fi}$ (yellow triangles) and the noble gases thermometry on another Milandre stalagmite *(24)* (M2, orange dots). Basel temperatures corrected for Fahy station (red arrow).

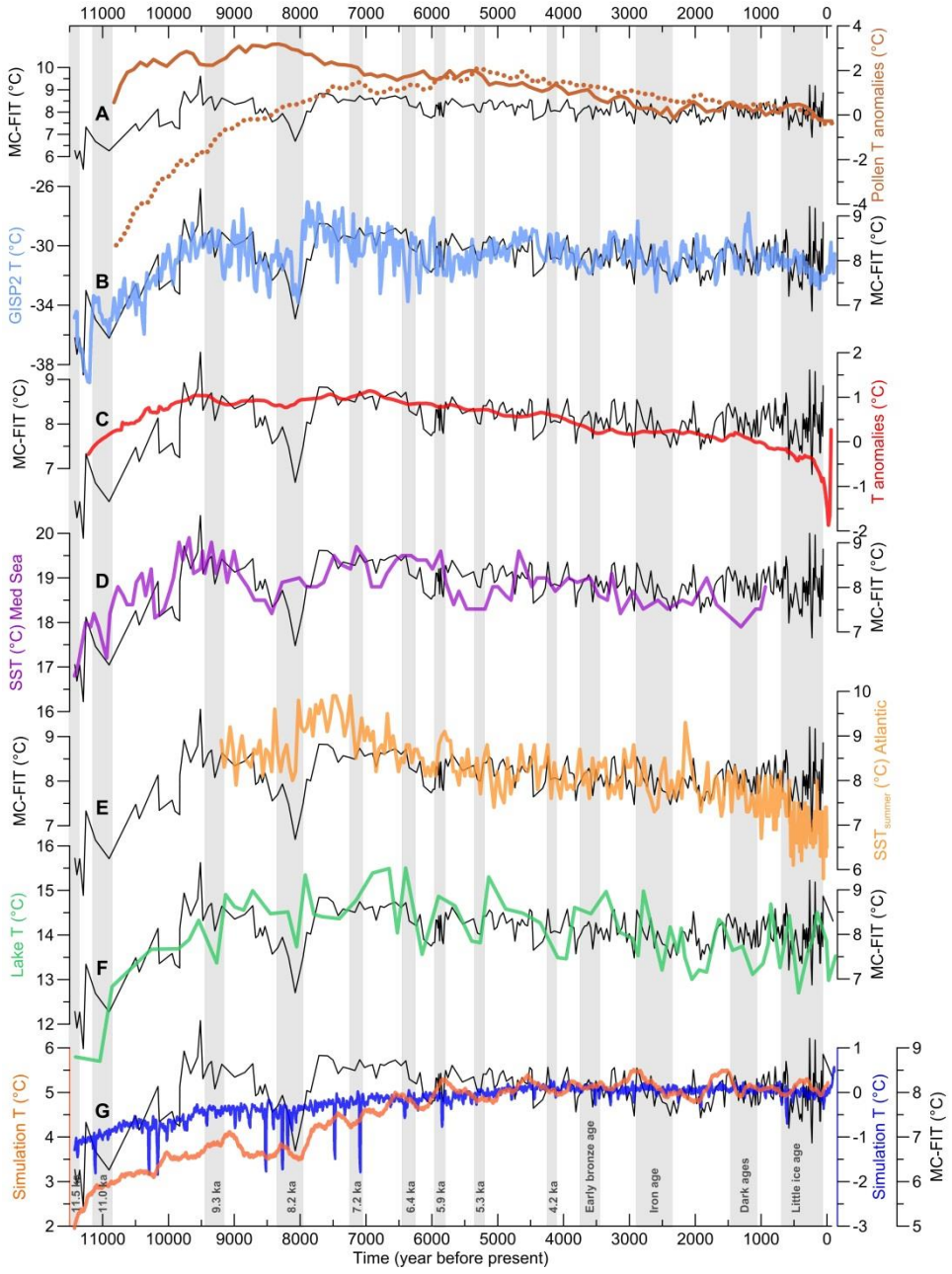

Fig. S7. Comparison of MC-FIT (black lines) with independent temperature records for the Holocene. (**A**) Regional pollen reconstruction for central Europe (43-49° N/5-13° E, brown) and northern Europe (53-62° N/18-27° E, dotted brown) *(4)* (**B**) Greenland temperature from GISP2 ice core *(11)*. (**C**) Multiproxy mean temperature anomalies *(2)*. (**D**) Mediterranean SST core MD95-2043 *(23)*. (**E**) Atlantic summer SST *(57)*. (**F**) Gemini lake July temperature *(9)*. (**G**) Model simulations showing regional (45-52° N; 2-12° E) CCSM3 temperatures *(3)* (orange) and LOVECLIM *(10)* temperature anomalies (blue) for Northern Hemisphere middle latitude (30-60° N). Shaded intervals correspond to Northern Hemisphere cold periods and events.

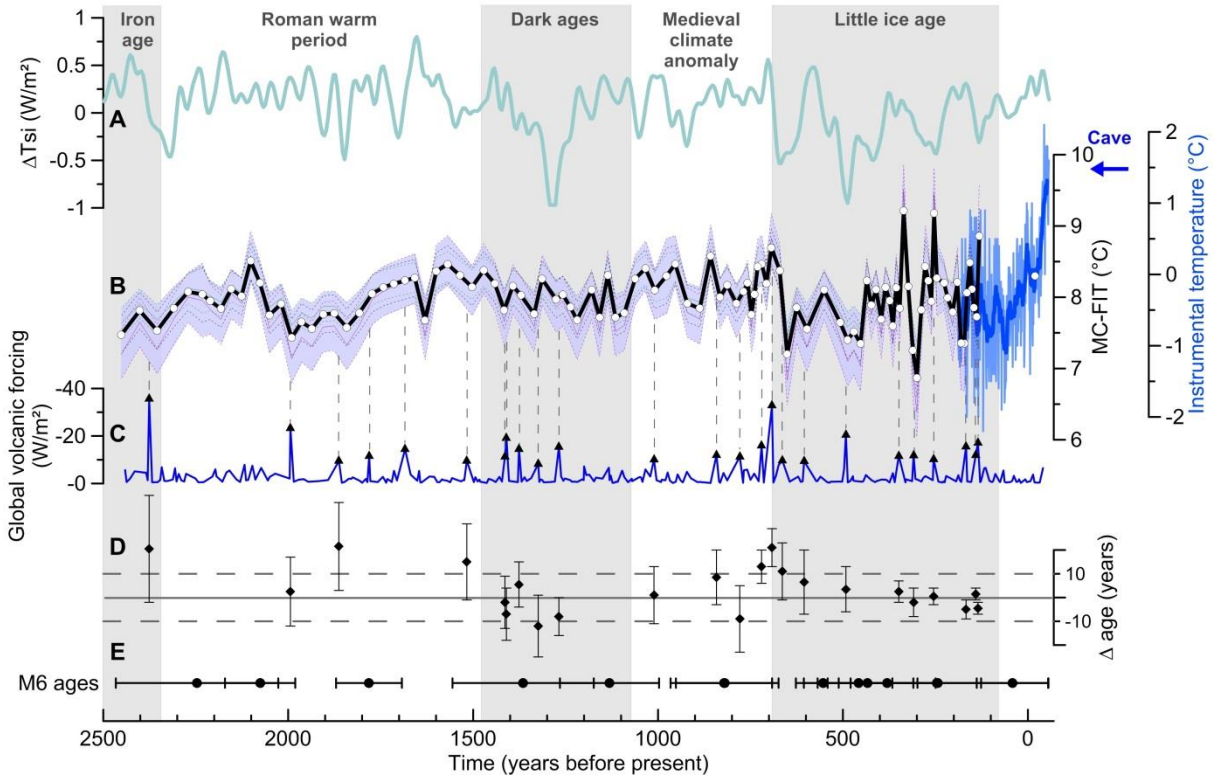

Fig. S8. Influence of volcanism on decadal temperature average. (**A**) Solar activity *(58)*. (**B**) Speleothem-based MC-FIT (black) with uncertainty range, instrumental mean annual air temperatures for the Swiss Plateau (light blue, 1760 – 2007 CE) and 11 years running mean (dark blue) (http://www.euroclimhist.unibe.ch/) and monitored cave temperature in 2012 – 2013 (blue arrow). (**C**) Major volcanic events of the last 2,500 years (black triangles) and global volcanic forcing *(36)* (blue). (**D**) Age offsets between eruption signals (time of cold year) and corresponding closest mean MC-FIT minima (black diamonds), error bars indicate the sample boundaries. (**E**) ^{230}Th ages and 2 sigma errors for M6 stalagmite. Shaded intervals correspond to Northern Hemisphere cold periods.

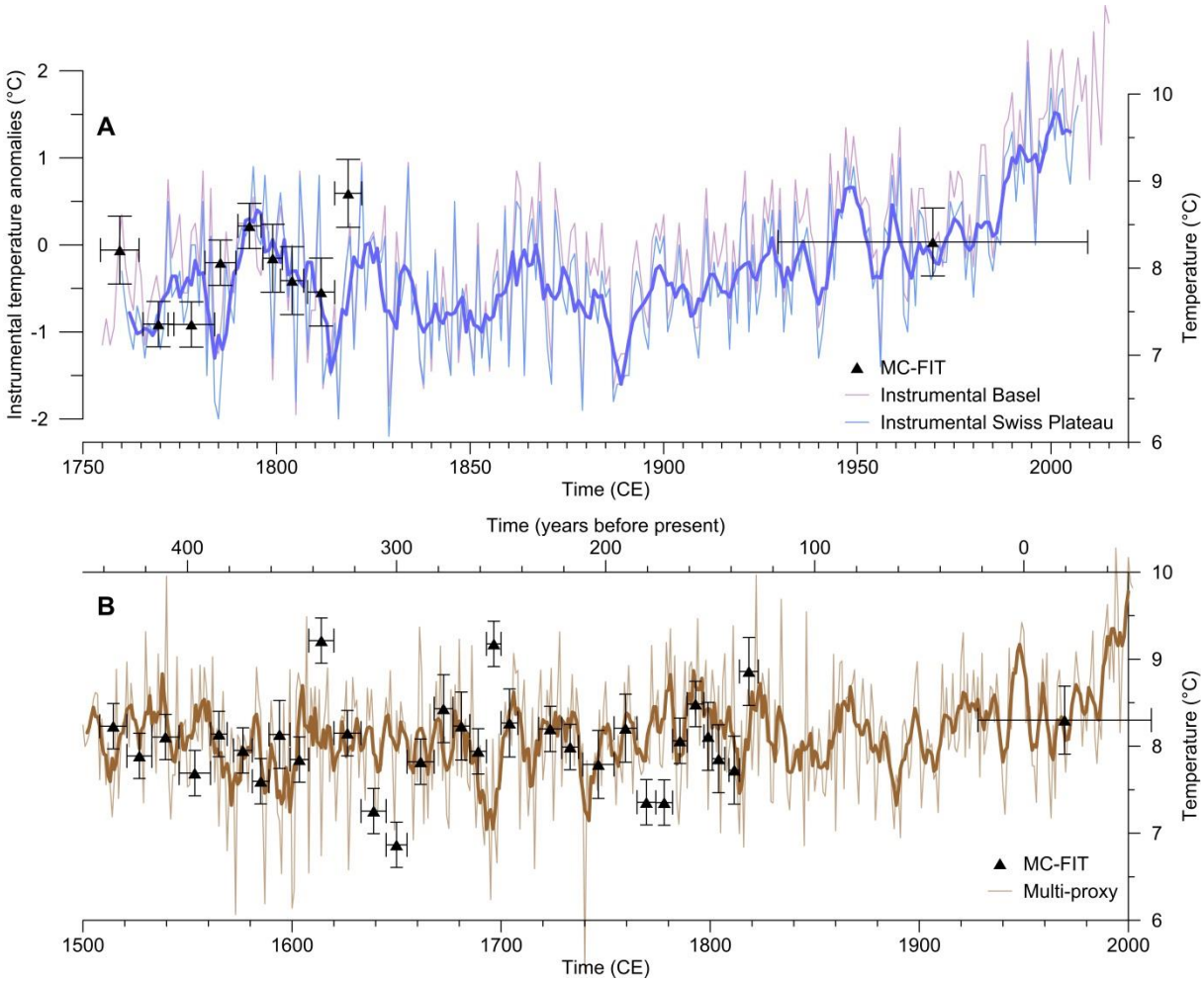

Fig. S9. Comparison between reconstructed (MC-FIT), instrumental, and multiproxy temperature records. (A) Speleothem MC-FIT record (black triangles), the given x-axis errors correspond to the sample age interval. Instrumental mean annual air temperature record for the Swiss Plateau (blue, 1760-2007 CE) and 5 years running average (bold blue) (http://www.euroclimhist.unibe.ch/). Also shown are temperature anomalies from Basel (rose, 1755-2015 CE). (B) Speleothem MC-FIT record (black triangles) and multi-proxy absolute annual temperature reconstruction for the Milandre Cave grid cell (brown) and 5 years running average (bold brown) *(29)*.

Table S1. ^{230}Th ages of M6 and M8 stalagmites from the Milandre Cave. The error is 2s error.

Sample Number	Depth (cm)	^{238}U (ppb)	^{232}Th (ppt)	^{230}Th / ^{232}Th (atomic x10^{-6})	δ^{234}U* (measured)	^{230}Th / ^{238}U (activity)	^{230}Th Age (yr) (uncorrected)	^{230}Th Age (yr) (corrected)	$\delta^{234}U_{Initial}$** (corrected)	^{230}Th Age (yr BP)*** (corrected)
M6_18	1.2	50.7 ±0.1	223 ±5	9 ±3	220.1 ±2.9	0.0023 ±0.0007	208 ±63	**103 ±97**	220 ±3	**41 ±97**
M6_25	7.3	46.1 ±0.1	809 ±16	8 ±1	224.5 ±1.6	0.0081 ±0.0004	724 ±39	**306 ±298**	225 ±2	**243 ±298**
M6_19	12.1	48.3 ±0.1	290 ±6	14 ±2	228.3 ±3.3	0.0051 ±0.0007	451 ±66	**308 ±120**	228 ±3	**246 ±120**
M6_24	17	48.9 ±0.1	365 ±7	15 ±1	230.6 ±2.5	0.0070 ±0.0004	620 ±40	**444 ±131**	231 ±2	**381 ±131**
M6_12	19.85	58.8 ±0.1	429 ±9	17 ±1	226.1 ±2.2	0.0075 ±0.0006	669 ±58	**495 ±135**	226 ±2	**433 ±135**
M6_20	22.4	51.8 ±0.1	139 ±3	47 ±4	219.8 ±3.6	0.0076 ±0.0007	679 ±59	**615 ±74**	220 ±4	**553 ±74**
M6_26	22.5	47.0 ±0.1	402 ±8	16 ±1	225.9 ±1.9	0.0081 ±0.0004	723 ±38	**521 ±148**	226 ±2	**458 ±148**
M6_29	27.5	37.7 ±0.1	308 ±6	24 ±1	217.2 ±2.1	0.0120 ±0.0005	1079 ±47	**883 ±146**	218 ±2	**820 ±146**
M6_21	29.5	47.0 ±0.1	298 ±6	30 ±2	215.7 ±3.3	0.0115 ±0.0008	1036 ±73	**884 ±130**	216 ±3	**822 ±130**
M6_27	34.7	45.1 ±0.1	340 ±7	33 ±1	221.9 ±1.9	0.0153 ±0.0005	1374 ±42	**1194 ±134**	223 ±2	**1131 ±134**
M6_10	40.35	41.6 ±0.1	426 ±9	30 ±2	227.6 ±3.2	0.0187 ±0.0009	1669 ±83	**1427 ±191**	229 ±3	**1365 ±191**
M6_17	47	60.8 ±0.1	233 ±5	93 ±3	222.8 ±2.3	0.0215 ±0.0007	1935 ±62	**1844 ±89**	224 ±2	**1782 ±89**
M6_28	52	46.1 ±0.1	233 ±5	82 ±2	215.4 ±1.9	0.0249 ±0.0005	2260 ±42	**2139 ±95**	217 ±2	**2076 ±95**
M6-35	55.6	64.7 ±0.1	825 ±17	37 ±1	210.8 ±1.4	0.0287 ±0.0004	2617 ±35	**2310 ±220**	212 ±1	**2246 ±220**
M6_32	56.75	50.2 ±0.1	662 ±13	47 ±1	218.4 ±2.3	0.0377 ±0.0007	3424 ±66	**3109 ±232**	220 ±2	**3046 ±232**
M6-36	60.8	58.5 ±0.1	655 ±13	50 ±1	211.3 ±1.9	0.0341 ±0.0007	3109 ±61	**2840 ±200**	213 ±2	**2776 ±200**
M6_16	62.4	62.6 ±0.1	687 ±14	53 ±2	213.6 ±2.7	0.0355 ±0.0008	3234 ±71	**2971 ±199**	215 ±3	**2909 ±199**
M6_9	68.45	65.3 ±0.1	447 ±9	95 ±2	208.2 ±3.0	0.0395 ±0.0007	3620 ±63	**3455 ±132**	210 ±3	**3393 ±132**
M6-37	70.3	60.5 ±0.1	811 ±16	52 ±1	207.2 ±2.3	0.0426 ±0.0006	3914 ±60	**3591 ±236**	209 ±2	**3527 ±236**
M6-38	77.2	51.8 ±0.1	1484 ±30	30 ±1	207.3 ±2.5	0.0517 ±0.0007	4770 ±64	**4078 ±494**	210 ±3	**4014 ±494**
M6_22	80.35	62.4 ±0.1	522 ±10	98 ±2	214.0 ±2.4	0.0500 ±0.0007	4577 ±65	**4376 ±156**	217 ±2	**4314 ±156**
M6-39	83.54	68.8 ±0.1	1196 ±24	52 ±1	203.2 ±3.1	0.0543 ±0.0006	5033 ±58	**4613 ±303**	206 ±3	**4549 ±303**
M6-40	87.1	62.3 ±0.1	1419 ±28	42 ±1	207.3 ±2.6	0.0573 ±0.0006	5299 ±59	**4750 ±393**	210 ±3	**4686 ±393**
M6_15	91.6	62.8 ±0.1	800 ±16	77 ±2	209.7 ±2.1	0.0596 ±0.0008	5506 ±75	**5200 ±229**	213 ±2	**5138 ±229**
M6-41	94.8	64.1 ±0.1	575 ±12	112 ±2	203.9 ±2.3	0.0613 ±0.0004	5689 ±41	**5473 ±159**	207 ±2	**5409 ±159**
M6_33	97.8	57.0 ±0.1	484 ±10	129 ±3	206.8 ±2.2	0.0664 ±0.0006	6158 ±61	**5953 ±157**	210 ±2	**5890 ±157**
M6-42	102.3	78.0 ±0.1	3316 ±67	29 ±1	206.7 ±2.2	0.0743 ±0.0006	6915 ±60	**5888 ±729**	210 ±2	**5824 ±729**

Sample Number	Depth (cm)	^{238}U (ppb)	^{232}Th (ppt)	^{230}Th / ^{232}Th (atomic x10^{-6})	$\delta^{234}U$* (measured)	^{230}Th / ^{238}U (activity)	^{230}Th Age (yr) (uncorrected)	^{230}Th Age (yr) (corrected)	$\delta^{234}U_{Initial}$** (corrected)	^{230}Th Age (yr BP)*** (corrected)
M6_14	105.3	84.1 ±0.2	842 ±17	114 ±3	211.6 ±3.1	0.0692 ±0.0006	6400 ±64	**6160 ±181**	215 ±3	**6098 ±181**
M6-43	109.1	70.1 ±0.1	1891 ±38	48 ±1	209.5 ±1.3	0.0781 ±0.0006	7269 ±57	**6620 ±462**	213 ±1	**6556 ±462**
M6_13	110.6	74.8 ±0.1	395 ±8	235 ±5	210.3 ±2.8	0.0750 ±0.0007	6964 ±67	**6838 ±111**	214 ±3	**6776 ±111**
M6-44	113.6	80.9 ±0.1	796 ±16	134 ±3	208.9 ±2.2	0.0802 ±0.0006	7468 ±57	**7232 ±176**	213 ±2	**7168 ±176**
M6_34	116	66.5 ±0.1	897 ±18	105 ±2	213.0 ±2.4	0.0859 ±0.0007	7989 ±70	**7666 ±239**	218 ±2	**7603 ±239**
M6-45	118.8	100.8 ±0.2	3047 ±61	51 ±1	212.1 ±2.6	0.0930 ±0.0006	8690 ±61	**7965 ±516**	217 ±3	**7901 ±516**
M6_11	121.6	85.5 ±0.2	277 ±6	474 ±10	221.1 ±3.3	0.0930 ±0.0008	8615 ±85	**8538 ±100**	227 ±3	**8476 ±100**
M6_23	125.95	80.0 ±0.1	541 ±11	237 ±5	210.5 ±2.2	0.0974 ±0.0006	9126 ±62	**8964 ±130**	216 ±2	**8902 ±130**
M6-46	127.6	82.9 ±0.1	5028 ±101	31 ±1	205.1 ±2.4	0.1147 ±0.0007	10877 ±74	**9411 ±1040**	211 ±3	**9347 ±1040**
M6_30	133.2	82.1 ±0.1	3723 ±75	42 ±1	205.8 ±1.7	0.1162 ±0.0007	11017 ±70	**9923 ±778**	212 ±2	**9860 ±778**
M6-47	134.8	103.2 ±0.2	2279 ±46	89 ±2	210.6 ±2.9	0.1188 ±0.0007	11230 ±72	**10701 ±381**	217 ±3	**10637 ±381**
M6-48	137.4	120.6 ±0.3	569 ±11	429 ±9	203.8 ±2.8	0.1229 ±0.0005	11704 ±61	**11591 ±101**	211 ±3	**11527 ±101**
M6-50	139.9	121.8 ±0.2	499 ±10	500 ±10	196.1 ±1.8	0.1242 ±0.0005	11924 ±57	**11825 ±90**	203 ±2	**11761 ±90**
M6-49	140.9	105.2 ±0.2	2027 ±41	114 ±2	199.9 ±2.4	0.1336 ±0.0006	12832 ±71	**12366 ±337**	207 ±3	**12302 ±337**
M6_31	144.7	225.4 ±0.3	4698 ±94	120 ±2	228.8 ±1.5	0.1522 ±0.0004	14364 ±48	**13873 ±351**	238 ±2	**13810 ±351**
M8-12	0.7	58.9 ±0.1	7373 ±148	10 ±1	205.3 ±2.5	0.0740 ±0.0008	6897 ±81	**3843 ±2164**	208 ±3	**3780 ±2164**
M8_1	1.5	72.5 ±0.1	4280 ±86	29 ±1	215.2 ±1.5	0.1053 ±0.0007	9856 ±70	**8440 ±1005**	220 ±2	**8377 ±1005**
M8-11	2.1	100.5 ±0.1	991 ±20	174 ±4	217.0 ±2.2	0.1040 ±0.0007	9720 ±68	**9486 ±179**	223 ±2	**9423 ±179**
M8-9	5.6	111.2 ±0.1	3414 ±68	63 ±1	221.8 ±1.7	0.1177 ±0.0006	11014 ±57	**10284 ±519**	228 ±2	**10221 ±519**
M8-10	5.7	115.2 ±0.1	9633 ±193	24 ±1	224.6 ±1.6	0.1209 ±0.0005	11298 ±54	**9303 ±1413**	231 ±2	**9240 ±1413**
M8-5	7.1	123.3 ±0.2	547 ±11	457 ±9	216.2 ±1.8	0.1232 ±0.0005	11610 ±48	**11504 ±89**	223 ±2	**11441 ±89**
M8-7	8.1	125.4 ±0.2	629 ±13	413 ±8	211.6 ±1.6	0.1255 ±0.0004	11886 ±48	**11767 ±97**	219 ±2	**11704 ±97**
M8-6	9.5	164.5 ±0.2	1127 ±23	335 ±7	224.5 ±1.7	0.1390 ±0.0004	13095 ±47	**12933 ±124**	233 ±2	**12870 ±124**
M8-8	10.7	173.7 ±0.3	1316 ±26	315 ±6	229.1 ±1.8	0.1450 ±0.0004	13632 ±48	**13454 ±135**	238 ±2	**13391 ±135**
M8_2	12.5	430.0 ±0.9	3244 ±65	359 ±7	312.5 ±2.0	0.1644 ±0.0006	14521 ±57	**14355 ±130**	325 ±2	**14292 ±130**
M8_3	14	63.5 ±0.1	3237 ±65	216 ±4	158.4 ±1.5	0.6690 ±0.0019	91571 ±438	**90333 ±977**	204 ±2	**90270 ±977**

U decay constants: $\lambda_{238} = 1.55125 \times 10^{-10}$ (Jaffey et al., 1971) and $\lambda_{234} = 2.82206 \times 10^{-6}$ (Cheng et al., 2013). Th decay constant: $\lambda_{230} = 9.1705 \times 10^{-6}$ (Cheng et al., 2013).

*$\delta^{234}U = ([^{234}U/^{238}U]_{activity} - 1) \times 1000$. ** $\delta^{234}U_{initial}$ was calculated based on ^{230}Th age (T), i.e., $\delta^{234}U_{initial} = \delta^{234}U_{measured} \times e^{\lambda 234 \times T}$.

Corrected ^{230}Th ages assume the initial $^{230}Th/^{232}Th$ atomic ratio of $4.4 \pm 2.2 \times 10^{-6}$. Those are the values for a material at secular equilibrium, with the bulk earth $^{232}Th/^{238}U$ value of 3.8. The errors are arbitrarily assumed to be 50%.

***B.P. stands for “Before Present” where the “Present” is defined as the year 1950 A.D.

Table S2. List of fix points. List of fix points (isotopic events) used for age model tuning in Milandre stalagmites, the corresponding depth in each sample (cm from top) for each event, together with the age and error assigned to each fix point (based on the M8 age model).

Tuning points			**Depth (cm from top)**	
Nr.	**Age (BP)**	**Error (2s)**	**M8**	**M6**
1	14454	176	12.8	145.16
2	14426	167	12.75	145.08
3	14372	151	12.65	144.98
4	14290	129	12.5	144.84
5	14237	120	12.4	144.7
6	13923	121	11.8	144.18
7	13872	126	11.7	144
8	13437	137	10.8	143.18
9	13414	134	10.75	142.88
10	13346	126	10.6	142.8
11	13224	104	10.3	142.64
12	13146	96	10.1	142.34
13	12870	120	9.5	142.08
14	12555	118	9.1	141.7
15	12458	110	9	141.52
16	11750	106	8.2	139.16
17	11703	98	8.1	138.88
18	11668	89	8	138.8
19	11591	68	7.7	138.52
20	11580	67	7.65	138.12
21	11538	65	7.45	137.98
22	11418	89	7.05	136.45
23	11297	106	6.85	135.95
24	11175	141	6.7	135.3
25	11083	178	6.6	135.15

Table S3. TF impact for different time interval.

Transfer function	‰/°C ($\delta^{18}O$)	‰/°C (δD)	T (°C)	Location	Interval	Tmin (°C)	Tmax (°C)
Long-term TF	0.60	4.80	0.6	Switzerland	Holocene (7787-1906 BP)	0.4	0.8
	0.60	4.80	4.3	Switzerland	YD-Holocene transition	4.1	4.5
	0.60		6.6	Greenland	YD-Holocene transition	6.4	6.8
Mean TF	0.48	3.84	0.7	Switzerland	Holocene (7787-1906 BP)	0.4	1.0
(~seasonal mean TF)	0.48	3.84	5.4	Switzerland	YD-Holocene transition	5.1	5.6
	0.48		8.2	Greenland	YD-Holocene transition	8.0	8.5
Monthly mean TF	0.36	2.88	0.9	Switzerland	Holocene (7787-1906 BP)	0.6	1.3
	0.36	2.88	7.2	Switzerland	YD-Holocene transition	6.8	7.5
	0.36		11.0	Greenland	YD-Holocene transition	10.6	11.3